

Interactions in electronic Mach-Zehnder interferometers with co-propagating edge channels

Luca Chirolli*,¹ Fabio Taddei,¹ Rosario Fazio,¹ and Vittorio Giovannetti¹

¹*NEST, Scuola Normale Superiore and Istituto Nanoscienze-CNR, I-56127 Pisa, Italy*

**luca.chirolli@sns.it*

We study Coulomb interactions in the finite bias response of Mach-Zehnder interferometers which exploit co-propagating edge states in the integer quantum Hall effect. Here, interactions are particularly important since the coherent coupling of edge channels is due to a resonant mechanism which is spoiled by inelastic processes. We find that interactions yield a saturation, as a function of bias voltage, of the period-averaged interferometer current which gives rise to unusual features, such as negative differential conductance, enhancement of the visibility of the current, non-bounded or even diverging visibility of the differential conductance.

PACS numbers: 73.43.-f, 71.10.Pm, 03.65.Yz, 85.35.Ds,

Introduction. — Topological edge states in the integer quantum Hall effect (IQHE) [1] represent an ideal playground for testing coherence of electronic systems at a fundamental level. Harnessing of edge states as quasi one-dimensional (1D) chiral electronic waveguides has allowed the successful realization of a number of electronic interferometric setups, such as Mach-Zehnder's [2–5] and Fabry-Perot-type's [6]. These devices exploit counter-propagating edge states localized at opposite sides of a Hall bar, which are brought in contact and mixed by quantum point constrictions (QPCs) that mimic the effect of optical Beam-Splitters (BSs). In Mach-Zehnder interferometer (MZI) setups the chirality of electron propagation makes it necessary the adoption of non simply-connected, Corbino-like geometries, which limit the flexibility of the devices. In these systems electron-electron (e-e) interactions are in general responsible for dephasing via the coupling with external edge channels [7, 8], which manifests as a reduction of the visibility of the Aharonov-Bohm (AB) oscillations as a function of the bias voltage. In particular, puzzling behaviors have been reported [3–5] in the finite bias response of MZIs, in which the visibility presents a lobe-like structure and phase-rigidity [7, 9–15].

An alternative MZI scheme inducing coherent mixing between edge states co-propagating at the *same* boundary of the sample, has been suggested [16] as a more flexible architecture, which allows multiple device concatenation [16, 17] and represents an ideal candidate for implementation of dual-rail quantum computation schemes [18, 19]. As schematized in Fig. 1, in such setup the BS transformations are now implemented through series of top gates, organized in arrays of periodicity λ tuned to compensate for the difference between the momenta of the co-propagating channels (the inner channel i and the outer channel o of the figure). The corresponding AB phase difference is introduced instead by separating the edge modes in the region between the two BSs through the action of a central, unmodulated, top gate

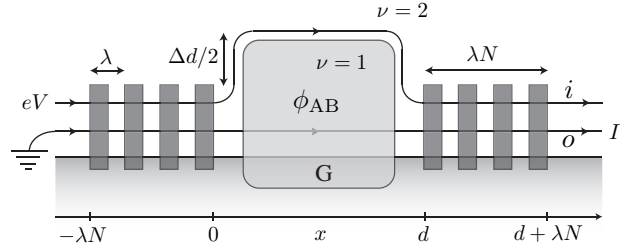


FIG. 1: Sketch of the MZI. Two sets of N top gates arranged in arrays with periodicity λ and separated by the distance d represent the L and R BSs of the interferometer. A central top gate G locally lowers the filling factor to $\nu = 1$ and separates the two edge states (i and o), which experience a path length difference Δd and acquire an AB phase ϕ_{AB} .

– see Refs. [16, 20, 21] for details. The effects of e-e interactions in this MZI are likely to be qualitatively different from those observed in the Corbino-like settings of Refs. [2–5]. Indeed, while in the latter the direct coupling between the channels that enter the interferometer can be neglected in the regions where they are coherently mixed (the QPCs), in the scheme of Fig. 1 this is no longer possible due to the non negligible spatial extension of the top gate arrays. This implies a strong interplay between coherent mixing and interactions which might impair the MZI response. Aim of the present work is to target such interplay. As detailed in the following, we show that the inter-edge current I measured at the output of the setup of Fig. 1 possesses a strong non-linear dependence in the bias voltage V that, while still exhibiting AB oscillations, leads to saturation of the associated mean value averaged over the AB phases. As a consequence the device presents negative differential conductance with unbounded visibility. Such anomalous behavior occurs since interactions enable inelastic scattering which spoils, for increasing voltages, the coherence needed for inter-edge coupling to occur at the BSs. Furthermore, as long as the interactions between the edge channels can be neglected

in the region between the two BSs, we also observe that for large voltages the visibility of current gets enhanced with respect to the non-interacting case.

Model: — Before discussing the role of e-e interactions in the device of Fig. 1, we find it useful to briefly review the basic properties of the scheme in the non-interacting case. The underlying idea [20] is to implement BS transformations between two co-propagating channels (i and o), via the action of a pair of arrays of top gates (see Fig. 1) which are spatially modulated at periodicity λ . Following Refs. [20, 21] we describe them through potentials of the form $t_L(x) = \bar{t}_L \sin^2(\pi x/\lambda)$, for $-\lambda N < x < 0$, and $t_R(x) = \bar{t}_R \sin^2(\pi(x-d)/\lambda)$, for $d < x < d + \lambda N$ (N being the number of elements of a single array while d being the distance between the two sets as measured according to the coordinates of the channel o). Introducing the difference $\Delta k = k_i - k_o$ between the momenta k_i and k_o of the two edges, the tunneling amplitude at a given BS can then be expressed as $\bar{t}_\alpha \text{sinc}(\lambda N(\Delta k - 2\pi/\lambda)/2)$, at lowest orders in \bar{t}_α (here $\alpha = L, R$ indicates the left and right BS, respectively) [20]. In this scenario Mach-Zhender interferences can be observed by introducing between the two BSs a top gate which locally lowers the filling factor to $\nu = 1$ and diverts the inner edge state toward the interior of the mesa [16]. This way, the two channels are guided along paths of difference lengths, $d_o = d$ and $d_i = d + \Delta d$, thus acquiring an AB phase difference ϕ_{AB} proportional to the magnetic field B and to the area enclosed by the path and a dynamical phase. The transmission probability $T(\epsilon)$ at energy ϵ of the MZI, from inner channel on the left to outer channel on the right, is then given by $T(\epsilon) \propto [|\bar{t}_L|^2 + |\bar{t}_R|^2 + 2|\bar{t}_L \bar{t}_R| \cos(\phi_{AB} + \epsilon \Delta d/v_F)] S^2$, where v_F is the group velocity of edge states and $S = \text{sinc}(\lambda N(\Delta k - 2\pi/\lambda)/2)$ is the BS amplitude which is optimal when the resonant condition $\Delta k = 2\pi/\lambda$ is met. A bias voltage V applied between channels i and o gives rise to a zero-temperature current $I(V) \propto \int_0^{eV} d\epsilon T(\epsilon)$, whose associated visibility $\mathcal{V}_I = (\max_\phi I - \min_\phi I)/(\max_\phi I + \min_\phi I)$ of the AB oscillations amounts to $\mathcal{V}_I = \mathcal{V}_\sigma^{(0)} |\text{sinc}(eV \Delta d/2v_F)|$, with $\mathcal{V}_\sigma^{(0)} = 2|\bar{t}_L \bar{t}_R|/(|\bar{t}_L|^2 + |\bar{t}_R|^2)$ being the oscillation visibility of the differential conductance $\sigma = dI/dV$.

To analyze the effect of interactions in such a set up we describe the linearly dispersing electronic excitations around the Fermi energy by means of two chiral fermion fields $e^{ik_m x} \psi_m(x)$, with $m = i, o$, each propagating at mean momentum k_m . The kinetic Hamiltonian can then be written as ($\hbar = 1$) $H_{\text{kin}} = -iv_F \sum_m \int dx \psi_m^\dagger \partial_x \psi_m$. The action of the BSs are instead assigned by means of the tunneling Hamiltonian $H_{\text{tun}} = \sum_{\alpha=L,R} (A_\alpha + A_\alpha^\dagger)$, where A_α describe the action of the gate arrays potentials and are defined as $A_L = \int dx t_L(x) e^{i\Delta k x} \psi_o^\dagger(x) \psi_i(x)$, $A_R = \int dx t_R(x) e^{i\Delta k x} \psi_o^\dagger(x) \psi_i(x + \Delta d)$ with $t_L(x)$, $t_R(x)$, and Δd introduced previously. In these expressions the local phase shift $e^{i\Delta k x}$ accounts for the reso-

nant behavior of the MZI. The AB phase of the setup (together with a dynamical phase term $k_i d_i - k_o d_o$) is instead included in the tunneling amplitude of the right beam-splitter, i.e. $\bar{t}_R \rightarrow e^{i\phi_{AB}} \bar{t}_R$.

As far as e-e interactions are concerned, an electron propagating in one edge channel can interact with all the electrons in the Fermi seas of both channels. Although the precise form of the interaction potential is unknown, screening provided by top gates makes it reasonable to assume a short range density-density interaction. The latter however needs not to be uniform in the whole sample: as a matter of fact, while intra-channel couplings are present everywhere, the inter-channel interactions depend on the edge channel spatial separation, which in our setup varies strongly from place to place (see Fig. 1). In particular in the region between the BSs edge states are brought far apart by the central top gate G and it is reasonable to assume the inter-channel coupling to be off. Inter-channel interactions, however, cannot be excluded in the regions before and after G, where the tunneling term H_{tun} is active. Indicating with $\rho_m = \psi_m^\dagger \psi_m$ the 1D density operator in channel $m = i, o$, we account for these effects by introducing an inter-channel e-e coupling $H_{\text{inter}} = \int dx \int dx' : \rho_o(x) U(x, x') \rho_i(x') :$ characterized by a coordinate dependent potential $U(x, x')$ which nullifies in the central top gate region (i.e. $0 \lesssim x \lesssim d$) and which approaches the short range behaviors $2\pi g \delta(x - x')$ and $2\pi g \delta(x - x' - \Delta d)$ on the lhs part (i.e. $x \lesssim 0$) and on the rhs part ($x \gtrsim d$) of the setup, respectively (the transition between these regions being smooth). In these expressions the interaction strength g has the dimension of a velocity while, similarly to H_{tun} , the parameter Δd accounts for the relative coordinate shift experienced by the inner edge with respect to the outer. A short range intra-channel coupling term of the form $H_{\text{intra}} = \pi u \sum_m \int dx : \rho_m^2(x) :$ is also considered (in this case however no coordinate dependence is assumed).

Methods: — Including the e-e interaction, the response of the interferometer driven out from equilibrium by a bias voltage $\mu_i - \mu_o = eV$ applied between the two edge states, will be analyzed at lowest order in the tunneling Hamiltonian H_{tun} (an exact analytical treatment being impossible). At second order in the amplitudes \bar{t}_α this allows to express the current flowing through the outer edge as $I(V) = e \sum_{\alpha,\beta} \int dt \langle [A_\alpha^\dagger(t), A_\beta(0)] \rangle$, where $A_\alpha(t) = e^{iH_0 t} A_\alpha e^{-iH_0 t}$ is the tunneling term evolved through the kinetic and interaction components of the system Hamiltonian, i.e. $H_0 = H_{\text{kin}} + H_{\text{intra}} + H_{\text{inter}}$, while expectation values are taken with respect to the ground state of the system biased by the chemical potential difference eV [7, 22].

Expanding the summation over α and β , we recognize the presence of three contributions: $I = I_L + I_R + I_\Phi$ with $I_\alpha = e \int dt \langle [A_\alpha^\dagger(t), A_\alpha(0)] \rangle$, for $\alpha = L, R$ being direct terms which do not depend upon the relative phase accumulated by the electrons when traveling through the

MZI, and with $I_\Phi = e \int dt \langle [A_L^\dagger(t), A_R(0)] \rangle + \text{c.c.}$ being a cross-term, which is sensitive to the AB phase. Explicit expressions for these quantities are obtained by means of the two-point electron and hole Green's functions $\mathcal{G}_m^e(x, t; x') = \langle \psi_m(x, t) \psi_m^\dagger(x', 0) \rangle$ and $\mathcal{G}_m^h(x, t; x') = \langle \psi_m^\dagger(x, t) \psi_m(x', 0) \rangle$, which we calculated by bosonization of the Hamiltonian H_0 . For this purpose we introduce chiral bosonic fields ϕ_m , which satisfy the commutation rules $[\phi_m(x), \phi_{m'}(x')] = i\pi\delta_{m,m'}\text{sign}(x-x')$ [23, 24] and express the fermion fields as $\psi_m = \frac{\hat{F}_m}{\sqrt{2\pi a}} e^{2\pi i \hat{N}_m x/L} e^{-i\phi_m}$ where a is a cutoff length that regularizes the theory at short wavelengths, \hat{F}_m are the Klein operators, $\hat{N}_m = \int dx : \rho_m(x) :$ are the total number operators of the edge states, while finally L is the edge quantization lengths. Observing that $\rho_m = (1/2\pi)\partial_x\phi_m + \hat{N}_m/L$, the kinetic and intra-channel Hamiltonian (apart for an irrelevant term proportional to $\sum_m \hat{N}_m$) becomes $H_{\text{kin}} + H_{\text{int}}^{\text{intra}} = (v/4\pi) \sum_m \int dx (\partial_x\phi_m)^2 + H_C^{\text{intra}}$ where $v = v_F + u$ is the renormalized edge group velocity [7, 12, 23], and where $H_C^{\text{intra}} = \pi v \sum_m \hat{N}_m^2/L$ is a capacitive contribution. Vice-versa, exploiting the smooth variation assumption of the potential $U(x, x')$ and the fact that L is the largest length in the problem, the inter-channel interaction term yields

$$H_{\text{int}}^{\text{inter}} \simeq g \int_{-\infty}^0 \frac{dx}{2\pi} (\partial_x\phi_o)(\partial_x\phi_i) + g \int_d^\infty \frac{dx}{2\pi} (\partial_x\phi_o(x))(\partial_x\phi_i(x + \Delta d)) + H_C^{\text{inter}}, \quad (1)$$

with $H_C^{\text{inter}} = (2\pi g/L)\hat{N}_o\hat{N}_i$ being a cross capacitive contribution. The Hamiltonian H_0 can now be brought to a diagonal form by solving the eigenvector equation $[H_0, \hat{\gamma}_\pm(\epsilon)] + \epsilon \hat{\gamma}_\pm(\epsilon) = 0$, which defines bosonic energy eigenmodes $\hat{\gamma}_\pm(\epsilon)$. Accordingly we obtain

$$\phi_m(x, t) = \int_0^\infty \frac{d\epsilon}{\sqrt{\epsilon}} e^{-i\epsilon(t-i\tau)} \sum_{s=\pm} \varphi_m^s(x, \epsilon) \hat{\gamma}_s(\epsilon) + \text{h.c.}, \quad (2)$$

where the wavefunctions φ_m^s satisfy the relation $\sum_s \int_0^\infty \frac{d\epsilon}{\epsilon} \text{Im}[\varphi_m^s(x, \epsilon) \varphi_{m'}^s(x', \epsilon)^*] = \frac{\pi}{2} \delta_{m,m'} \text{sign}(x-x')$, and $1/\tau > 0$ is an energy cutoff related to a via the non-interacting dispersion $\epsilon = v_F q$, i.e. $a/\tau = v_F$. Solving the equations of motion by requiring only continuity of the wave functions we find $\varphi_m^\pm = f_\pm(x)$ for $x < 0$, $\varphi_m^\pm = C_\pm e^{i\epsilon x/v}$ for $0 < x < d_m$, with $C_+ = 1$, $C_- = 0$, and $\varphi_m^\pm = e^{i\epsilon d_m/v} f_\pm(x - d_m)$ for $x > d_m$, in terms of the symmetric and antisymmetric combinations $f_\pm(x) = (e^{i\epsilon x/v_+} \pm e^{i\epsilon x/v_-})/2$. Two new velocities enter the problem, a fast charged mode which propagates at $v_+ = v + g$ and a slow neutral mode which propagates at $v_- = v - g$. Exploiting these results, the electron and hole Green's functions can be finally written as $\mathcal{G}_m^e = e^{-i\mu_m(t-(x-x')/v_-)} \mathcal{G}_m(x, t; x')$ and $\mathcal{G}_m^h = e^{i\mu_m(t-(x-x')/v_-)} \mathcal{G}_m(x, t; x')$, with the zero-bias Green's function $\mathcal{G}_m(x, t; x') = \frac{1}{2\pi a} \langle e^{i\phi_m(x,t)} e^{-i\phi_m(x',0)} \rangle$,

which, thanks to the quadratic nature of the bosonized Hamiltonian H_0 , can be easily computed in terms of the wave functions φ_m^s . In particular to compute the direct current terms I_L and I_R we only need the correlation functions in the BS regions: $x, x' < 0$ for the left BS, and $x, x' > d_m$ for the right BS. At zero temperature, for these combinations we find

$$\mathcal{G}_m = \frac{i}{2\pi v_F} \prod_{s=\pm} \frac{1}{\sqrt{(x-x')/v_s - \tilde{t}}}, \quad (3)$$

(here $\tilde{t} = t - i\tau$). The term I_Φ is obtained instead through crossed combinations. In particular for $x > d_m$ and $x' < 0$ we get

$$\mathcal{G}_m = \frac{i}{2\pi v_F} \prod_{s=\pm} \frac{1}{\sqrt{(x-x')/v_s + d_m(1/v - 1/v_s) - \tilde{t}}}, \quad (4)$$

and analogously for $x' > d_m$ and $x < 0$, with the replacement $d_m \rightarrow -d_m$.

Currents: — With the help of Eqs. (3) and (4) the I - V characteristics of the setup can now be explicitly computed. In particular for the direct contributions of the current one gets

$$I_\alpha(V) = \frac{e}{2\pi} n_F^2 |\bar{t}_\alpha|^2 \int_0^{eV} d\epsilon S^2(\epsilon/\epsilon_c), \quad (5)$$

with the resonance function $S(x) = \text{sinc}(\lambda N(\Delta k - 2\pi/\lambda)/2 - x/2)$, and the density of states at the Fermi energy $n_F = \lambda N/(2v_F)$. The energy scale $\epsilon_c = (\lambda N(1/v_- - 1/v_+))^{-1}$ is associated to the difference in time-of-flight for propagation of the bosonic excitations at speeds v_+ and v_- through the BS of length λN : in the absence of interactions it diverges. We notice that while for a low bias I_α is linear in V , for a bias larger than ϵ_c it saturates to the constant value $I_\alpha^{\text{asy}} = \pi G_0 n_F^2 |\bar{t}_\alpha|^2 \epsilon_c$. This is shown by the dashed lines in Fig. 2, top panel, where I_α is plotted as a function of V for different values of g . Such behavior is due to the fact that inelastic processes, which are induced by the interaction and increase with increasing voltage bias, spoil the resonant coherent effect which is responsible for the transfer of charges between the two edge channels in the BS, thus suppressing I_α .

The cross term contribution I_Φ to the current is obtained instead through integration over the branch cuts [12] of the Green's functions (4). Introducing

$$\mathcal{A} = \int_0^{eV} d\epsilon e^{i\varphi_V(\epsilon)} S^2(\epsilon/\epsilon_c) J_0 \left[\frac{\epsilon}{2\epsilon_{\text{dyn}}} \right] J_0 \left[\frac{eV - \epsilon}{2\epsilon_{\text{dyn}}} \right], \quad (6)$$

together with the phase $\varphi_V(\epsilon) = \epsilon/\epsilon_c + (\Delta k - 2\pi/\lambda)\lambda N + eV[\Delta d/(2v_-) + (d + \Delta d/2)(1/v - 1/v_-)]$, we obtain

$$I_\Phi(V) = \frac{e}{2\pi} n_F^2 2|\bar{t}_L \bar{t}_R| |\mathcal{A}| \cos(\phi_{\text{AB}} + \arg(\mathcal{A})), \quad (7)$$

where $J_0[x]$ is the Bessel function of the first kind and $\epsilon_{\text{dyn}} = v/\Delta d$. The latter is a new energy scale associated

to the dynamical phase difference acquired by the electrons in the interference region between the BSs, where inter-channel interaction is absent and excitations move at speed v . Due to the bias dependence of $\arg(\mathcal{A})$, the current I_{Φ} shows oscillations versus bias around zero.

The overall I - V characteristics (full lines plotted for different values of g in Fig. 2, top panel) show an oscillating behavior which becomes non-monotonic for large values of the bias V . The associated visibility is $\mathcal{V}_I(V) = \mathcal{V}_{\sigma}^{(0)} |\mathcal{A}| / \int_0^{eV} d\epsilon S^2(\epsilon/\epsilon_c)$, where $\mathcal{V}_{\sigma}^{(0)}$, as in the absence of interactions, provides the upper bound ($\mathcal{V}_I \leq \mathcal{V}_{\sigma}^{(0)} \leq 1$). Plots of $\mathcal{V}_I(V)$ for different values of g are shown in the bottom panel of Fig. 2. For $g/v_F = 0.1$ (red curve), weakly interacting regime, $\mathcal{V}_I(V)$ closely follows the non-interacting case (black curve) for $V \leq V^* = 2\pi\hbar v_F/(e\Delta d)$ and thereafter oscillating without reaching zero. In the strongly interacting regime $g \gg v_F$, the scale ϵ_c already dominates at relatively low biases, leading to a completely different behavior. As shown by the blue curve ($g/v_F = 10$), $\mathcal{V}_I(V)$ decreases with the bias very rapidly up to $eV \leq \epsilon_c$ and very slowly thereafter (with the parameters used in the plot $\epsilon_c/(eV^*) \simeq 0.32$). The almost constant value exhibited by the curve is the consequence of the fact that the current oscillates around a constant value, with amplitude of oscillations that decreases very slowly with bias. Interestingly, in this regime the visibility in the interacting case is higher than in the non-interacting case. Very peculiar is also the case of a symmetric interferometer, $\Delta d = 0$, where ϵ_{dyn} diverges and the visibility becomes $\mathcal{V}_I^{\Delta d=0} = \mathcal{V}_{\sigma}^{(0)} |\mathcal{F}_2(V)|/\mathcal{F}_0(V)$, where $\mathcal{F}_p(V) = \int_0^{eV/(2\epsilon_c)} dx e^{ixp} \text{sinc}^2(x)$. We find that the ratio $\mathcal{V}_I^{\Delta d=0}/\mathcal{V}_{\sigma}^{(0)}$ goes, for $eV \gg \epsilon_c$, asymptotically to the finite value $2\ln(2)/\pi$. Therefore, a symmetric device over-performs with respect to an asymmetric one for large voltages.

The highly non-monotonic behavior of $I(V)$ detailed above is best understood by studying the differential conductance dI/dV . In particular, its direct contribution amounts to $\frac{dI_{\alpha}}{dV} = \frac{e}{2\pi} n_F^2 |\bar{t}_{\alpha}|^2 S^2(eV/\epsilon_c)$, and it shows how e-e interactions effectively give rise to an interaction- and bias-dependent shift of the resonance condition

$$\Delta k = \frac{2\pi}{\lambda} + \frac{2g}{v_+ v_-} eV. \quad (8)$$

As a result, dI_{α}/dV becomes negligible beyond an applied voltage on order of ϵ_c , which explains the saturation of the period-averaged current in Fig. 2 in the strongly interacting regime (notice also that for weak interaction the applied bias voltage V allows for fine tuning of the resonance condition). At the same time a non-negligible cross term dI_{Φ}/dV results in an overall behavior of the total differential conductance dI/dV which exhibits regions of negative values. Furthermore, while the associated visibility of the AB oscillations in the presence of interactions is known to exhibit values larger than one [12],

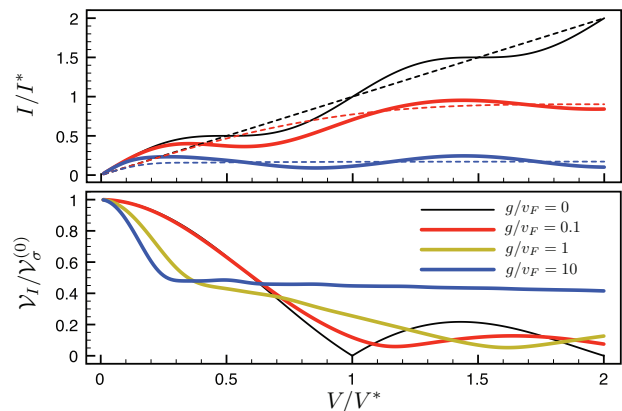


FIG. 2: (Color online) Response of the MZI versus bias V [in units of $V^* = 2\pi\hbar v_F/(e\Delta d)$] for different values of the interaction parameter g/v_F . We have assumed $u = g$, $\phi_{AB} = 0$, $|\bar{t}_L| = |\bar{t}_R| = |\bar{t}|$ and that the resonant condition, $\Delta k = 2\pi/\lambda$, is satisfied. Top panel: total current I (full curves) and BS current (dashed curves) in units of $I^* = 2n_F^2 |\bar{t}|^2 e^2 V^*/h$. Bottom panel: Visibility of the AB oscillations in the current \mathcal{V}_I in units of $\mathcal{V}_{\sigma}^{(0)}$. According to Ref. [20], we set $\lambda N/\Delta d = 3$ and $d/\Delta d = 1$.

for our setup this quantity diverges for values of bias V such that the direct contributions to the differential conductance vanishes.

Conclusions. — The analysis presented in this paper confirms for a MZI with co-propagating edge states the picture in which electron-electron interaction in general reduces the performances of an electronic interferometer. There are, however, striking differences with respect to non-simply connected MZI architectures. In the latter case interactions couple the interferometer edge channels to additional channels that carry information away from the system [3–5, 12]. In our setup interactions directly couple the two interferometer edge states and information is redistributed in the system. The major impact of interaction effects is the spoiling of the resonant single-particle tunneling, that realizes the BS, while the oscillating component of the interferometer current is only marginally affected because inter-edge interactions are negligible in the interference region. This leads to the unexpected result that strong interactions yield a reduction of the current visibility for small voltages, but an enhancement for larger voltages, with respect to the non-interacting case. Furthermore, the differential conductance can become negative in some voltage range, while its visibility can take large values or even diverge.

Acknowledgments. — We thank B. Karmakar for useful discussions. This work has been supported by the EU FP7 Programme under Grant Agreement No. 234970-NANOCTM, No. 248629-SOLID, No. 233992-QNEMS, No. 238345-GEOMDISS, and No. 215368-SEMISPINNET.

-
- [1] *The Quantum Hall Effect*, edited by R. E. Prange and S. M. Girvin (Springer, New York, 1987).
- [2] Y. Ji, Y. Chung, D. Sprinzak, M. Heiblum, D. Mahalu, and H. Shtrikman, *Nature (London)* **422**, 415 (2003).
- [3] I. Neder, M. Heiblum, Y. Levinson, D. Mahalu, and V. Umansky, *Phys. Rev. Lett.* **96**, 016804 (2006).
- [4] P. Roulleau, F. Portier, D. C. Glattli, P. Roche, A. Cavanna, G. Faini, U. Gennser, and D. Mailly, *Phys. Rev. B* **76**, 161309(R) (2007).
- [5] L. V. Litvin, H.-P. Tranitz, W. Wegscheider, and C. Strunk, *Phys. Rev. B* **75**, 033315 (2007); L. V. Litvin, A. Helzel, H.-P. Tranitz, W. Wegscheider, and C. Strunk, *ibid.* **78**, 075303 (2008).
- [6] D. T. McClure, Y. Zhang, B. Rosenow, E. M. Levenson-Falk, C. M. Marcus, L. N. Pfeiffer, and K. W. West, *Phys. Rev. Lett.* **103**, 206806 (2009).
- [7] J. T. Chalker, Yuval Gefen, and M. Y. Veillette, *Phys. Rev. B* **76**, 085320 (2007).
- [8] C. Neuenhahn and F. Marquardt, *Phys. Rev. Lett.* **102**, 046806 (2009).
- [9] E. V. Sukhorukov and V. V. Cheianov, *Phys. Rev. Lett.* **99**, 156801 (2007).
- [10] I. Neder, E. Ginossar, *Phys. Rev. Lett.* **100**, 196806 (2008).
- [11] S.-C. Youn, H.-W. Lee, H.-S. Sim, *Phys. Rev. Lett.* **100**, 196807 (2008).
- [12] I. P. Levkivskyi and E. S. Sukhorukov, *Phys. Rev. B* **78**, 045322 (2008).
- [13] I. P. Levkivskyi and E. V. Sukhorukov, *Phys. Rev. Lett.* **103**, 036801 (2009).
- [14] D. L. Kovrizhin and J. T. Chalker, *Phys. Rev. B* **80**, 161306(R) (2009); *ibid.* **81**, 155318 (2010).
- [15] M. J. Rufino, D. L. Kovrizhin and J. T. Chalker, arXiv:1209.1127 (2012).
- [16] V. Giovannetti, F. Taddei, D. Frustaglia, and R. Fazio, *Phys. Rev. B* **77**, 155320 (2008).
- [17] L. Chirolli, E. Strambini, V. Giovannetti, F. Taddei, V. Piazza, R. Fazio, F. Beltram, and G. Burkard *Phys. Rev. B* **82**, 045403 (2010).
- [18] I. L. Chuang and Y. Yamamoto, *Phys. Rev. A* **52**, 3489 (1995).
- [19] E. Knill, R. Laflamme, and G. J. Milburn, *Nature (London)* **409**, 46 (2001).
- [20] B. Karmakar, D. Venturelli, L. Chirolli, F. Taddei, V. Giovannetti, R. Fazio, S. Roddaro, G. Biasiol, L. Sorba, V. Pellegrini, F. Beltram, *Phys. Rev. Lett.* **107**, 236804 (2011).
- [21] L. Chirolli, D. Venturelli, F. Taddei, R. Fazio, and V. Giovannetti, *Phys. Rev. B* **85**, 155317 (2012).
- [22] E. Sukhorukov, G. Burkard, D. Loss, *Phys. Rev. B* **63**, 125315 (2001).
- [23] J. von Delft and H. Schöller, *Ann. Phys. (Leipzig)* **7**, 225 (1998).
- [24] T. Giamarchi, *Quantum Physics in One Dimension*, Oxford University Press, Oxford, England (2004).